

See discussions, stats, and author profiles for this publication at: <https://www.researchgate.net/publication/51845392>

# Bacterial and Viral Sialidases: Contribution of the Conserved Active Site Glutamate to Catalysis

ARTICLE *in* BIOCHEMISTRY · DECEMBER 2011

Impact Factor: 3.02 · DOI: 10.1021/bi201019n · Source: PubMed

---

CITATIONS

7

---

READS

45

6 AUTHORS, INCLUDING:



Jefferson Chan

University of Illinois, Urbana-Champaign

23 PUBLICATIONS 433 CITATIONS

SEE PROFILE

# Bacterial and Viral Sialidases: Contribution of the Conserved Active Site Glutamate to Catalysis

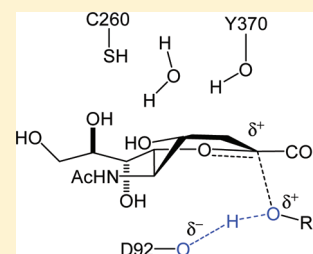
Jefferson Chan,<sup>†</sup> Jacqueline N. Watson,<sup>†,§</sup> April Lu,<sup>†</sup> Viviana C. Cerda,<sup>‡</sup> Thor J. Borgford,<sup>†,||</sup> and Andrew J. Bennet<sup>\*,†</sup>

<sup>†</sup>Department of Chemistry, Simon Fraser University, 8888 University Drive, Burnaby, British Columbia V5A 1S6, Canada

<sup>‡</sup>Department of Molecular Biology and Biochemistry, Simon Fraser University, 8888 University Drive, Burnaby, British Columbia V5A 1S6, Canada

## S Supporting Information

**ABSTRACT:** Mutagenesis of the conserved glutamic acid of influenza type A (E277) and *Micromonospora viridifaciens* (E260) sialidases was performed to probe the contribution of this strictly conserved residue to catalysis. Kinetic studies of the E260D and E260C *M. viridifaciens* mutant enzymes reveal that the overall mechanism of action has not changed. That is, the mutants are retaining sialidases in which glycosylation and deglycosylation are rate-limiting for  $k_{\text{cat}}/K_m$  and  $k_{\text{cat}}$ , respectively. The solvent kinetic isotope effect and proton inventory on  $k_{\text{cat}}$  for the E260C mutant sialidase provide strong evidence that the newly installed cysteine residue provides little catalytic acceleration. The results are consistent with the conserved aspartic acid residue (D92) becoming the key general acid/base residue in the catalytic cycle. In addition, the E277D mutant influenza type A sialidase is catalytically active toward 4-nitrophenyl  $\alpha$ -D-sialoside, although no measurable hydrolysis of natural substrates was observed. Thus, mutating the glutamate residue (E277) to an aspartate increases the activation free energy of hydrolysis for natural substrates by >22 kJ/mol.



Sialidases are retaining glycosidases<sup>1,2</sup> that catalyze hydrolysis of *N*-acetylneuraminic acid residues  $\alpha$ -linked to glycoconjugates.<sup>3,4</sup> Sialidases have been classified into three glycosyl hydrolase families (GH) on the basis of bioinformatic analyses of amino acid sequences and predicted structural similarities.<sup>5</sup> Influenza viral sialidases are in family GH 34; the bacterial and eukaryotic enzymes are in family GH 33,<sup>5–7</sup> while the human parainfluenza virus dual-function hemagglutinin-neuraminidase enzymes are found in GH 83. All of these families belong to clan GH-E, which contains a six-fold  $\beta$ -propeller as the prominent structural motif. The most thoroughly examined viral and bacterial sialidases are those from influenza type A (GH 34) and *Micromonospora viridifaciens* (GH 33), respectively. In the case of influenza viruses, the presence of the *exo*-sialidase is essential for the release of progeny virus particles from infected cells.<sup>8</sup> In contrast, the *M. viridifaciens* enzyme is expressed in various forms, depending on the type of substrate available; it serves to release sialic acids from soil glycoconjugates, which can then be used as a carbon source.<sup>9,10</sup>

In all cases, the active site of *exo*-sialidase enzymes contains three acidic amino acids, a tyrosine, and three arginines,<sup>11</sup> where the key residues involved in catalysis are an aspartic acid, a glutamic acid, and the tyrosine residue.<sup>12–14</sup> For the enzyme from the influenza type A Tokyo 3/67 strain, Tyr-406 is the catalytic nucleophile while Asp-151 and Glu-277 are believed to perform general acid/base catalytic roles. The corresponding residues for the *M. viridifaciens* enzyme are Tyr-370, Asp-92, and Glu-260, respectively (Figure 1).

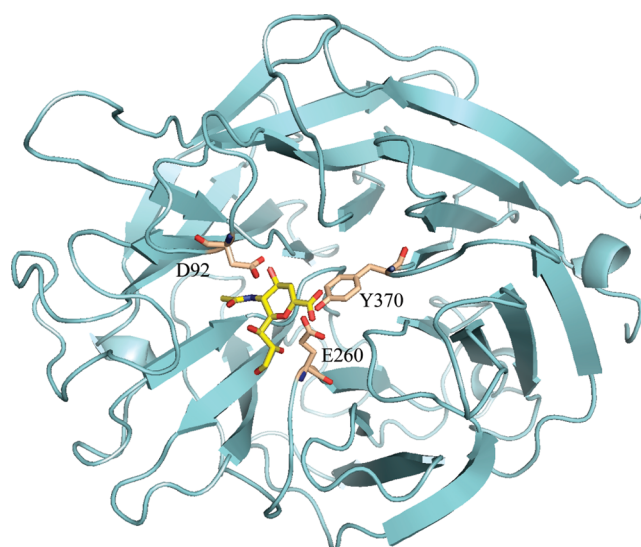


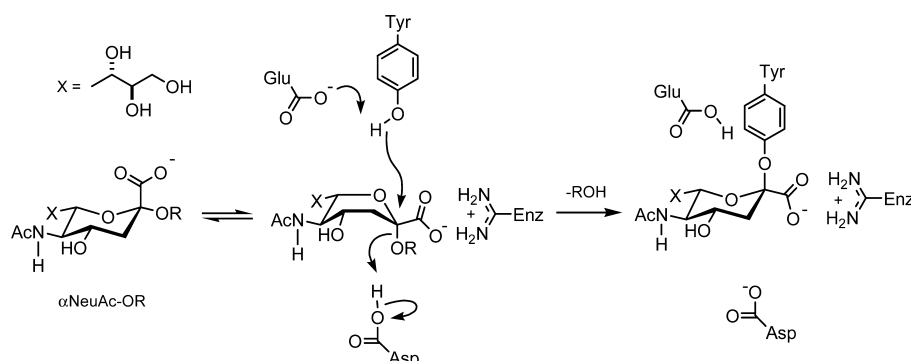
**Figure 1.** Active site (Y370, E260, and D92) residues of the *M. viridifaciens* wild-type sialidase (Protein Data Bank entry 1EUS) and the bound inhibitor Neu2en5Ac (DANA), which is represented with a yellow carbon skeleton. The equivalent residues in the influenza A sialidase that was studied are Y406, E277, and D151, respectively.

Received: July 3, 2011

Revised: November 29, 2011

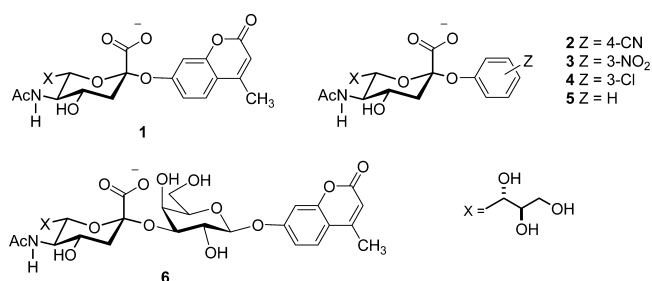
Published: December 1, 2011

**Scheme 1.** Proposed Mechanism of Glycosylation in Sialidases in Which the Glutamate Residue Is Presumed To Act as a General Base Catalyst Assisting the Nucleophilic Attack of the Active Site Tyrosine



The current mechanism, which is a refinement of several previous proposals,<sup>15–17</sup> for glycosylation is shown in Scheme 1.<sup>18–21</sup> The subsequent deglycosylation step involves the microscopic reverse reaction, but with attack by H<sub>2</sub>O rather than return of the aglycone leaving group (ROH). A previously postulated mechanism involving formation of a carbocationic intermediate<sup>13,22</sup> is now considered to be unlikely.

This study details the kinetic characterization, using a variety of sialoside substrates (1–6), of mutant sialidases from *M. viridifaciens* and influenza type A, in which the active site glutamic acid residue has been replaced with several different residues using site-directed mutagenesis. The two enzymes were chosen because the enzyme from influenza is the target for the drugs that are being stockpiled for the outbreak of a pandemic,<sup>23</sup> whereas the sialidase, and active site mutants thereof, from the soil bacterium *M. viridifaciens* is currently the best characterized.<sup>18–21,24–29</sup>



## MATERIALS AND METHODS

**Materials.** All restriction endonucleases and DNA modification enzymes were purchased from Gibco BRL or New England BioLabs. All DNA manipulations were conducted according to standard procedures.<sup>30</sup> Synthetic oligonucleotides were synthesized by the NAPS Unit of the University of British Columbia (Vancouver, BC). All chemicals were of analytical grade or better and were purchased from Sigma-Aldrich unless otherwise noted. MU- $\alpha$ Neu5Ac was purchased from Rose Scientific. Phenyl  $\alpha$ -D-N-acetylneuraminide was purchased from Sigma-Aldrich. 4-Cyanophenyl, 3-nitrophenyl, and 3-chlorophenyl  $\alpha$ -D-N-acetylneuraminides were synthesized according to literature procedures.<sup>31</sup> 3'-MUG- $\alpha$ Neu5Ac was prepared according to the method of Indurugalla et al.<sup>24</sup> All substrates (both commercial and synthesized) were estimated to be >95% pure by <sup>1</sup>H NMR spectroscopy. The *Aspergillus oryzae* and *Escherichia coli*  $\beta$ -galactosidases were purchased from Sigma-Aldrich.

***M. viridifaciens* Sialidase Mutagenesis.** The site-directed mutagenesis of the E260 codon in the wild-type *M. viridifaciens*

sialidase gene (pJWHS2) has been described previously.<sup>29</sup> Restriction and DNA sequence analysis was used to confirm the mutation, as well as to ensure that spurious mutations had not occurred during DNA manipulation. Sequencing primers included MV1415' (5'-CGG ACC CGG GCT GGC GC-3') and Y370A-R'.<sup>18</sup> Subsequently, the mutant sialidase genes for E260D and E260C were subcloned, respectively, into a C-terminal His tag sialidase construct by digesting each mutant plasmid (pJWHS-Ed3 and pJWHS-Ec1, respectively) with AgeI and MscI to yield a 794 bp product, which was then ligated into similarly digested and dephosphorylated pJW-OSH.<sup>21,29</sup> The subcloning step was verified by restriction analyses.

***M. viridifaciens* Sialidase Expression and Purification.** Expression of the E260D and E260C *M. viridifaciens* sialidase mutants was performed as described previously.<sup>21</sup> At 42 h postinduction, the culture supernatant (90 mL) was collected, filtered (0.22  $\mu$ m), and applied to a brand new His GraviTrap column [40 mg capacity (GE Healthcare)]. The column was washed with 16 mL of 10 mM imidazole and 20 mM sodium phosphate buffer (pH 7.4). The sialidase protein was eluted with 10 mL of 100 mM imidazole and 20 mM sodium phosphate buffer (pH 7.4). Purity was assessed by sodium dodecyl sulfate–polyacrylamide gel electrophoresis (SDS–PAGE). The purified mutant proteins were exchanged into storage buffer [10 mM Tris-HCl and 150 mM NaCl (pH 7.17)] and concentrated to approximately 1 mL using an Amicon Ultra-4 centrifugal filter [4 mL, 30 kDa molecular mass cutoff (Millipore)]. Aliquots of pure enzyme were stored at –80 °C. Total protein concentrations were determined by the Bradford assay using bovine serum albumin as the protein standard.

**Influenza Viral Sialidase Mutagenesis.** Plasmid pJW1<sup>32</sup> was used as the template for the A/Tokyo/3/67 sialidase gene. Substitution of the codon for residues D151 and E277 involved making mutations in both strands in two separate polymerase chain reaction experiments. All five mutants were created in a similar fashion. The front of the gene was amplified using the universal forward primer M13F' with a reverse mutagenic primer (mutated codons are underlined): D151A-R' (5'-CGA TGA GGG ATT CTA GCA TGT AC-3'), D151G-R' (5'-CGA TGA GGG ATT CTA CCA TGT AC-3'), D151N-R' (5'-CGA TGA GGG ATT CTG TTA TGT AC-3'), E277D-R' (5'-GAT AAC AGG AAC AAT CCT CTA C-3'), or E277Q-R' (5'-GAT AAC AGG AAC ACT GCT CTA C-3'). The back portion of the gene was amplified using the universal reverse primer M13R' and a forward mutagenic primer: D151A-F' (5'-CAT GCT AGA ATC CCT CAT CGA AC-3'), D151G-F' (5'-CAT

GGT AGA ATC CCT CAT CGA AC-3'), D151N-F' (5'-CAT AAC AGA ATC CCT CAT CGA AC-3'), E277D-F' (5'-GAG GAT TGT TCC TGT TAT CCT C-3'), or E277Q-F' (5'-GAG CAG TGT TCC TGT TAT CCT C-3'). The front and back fragments had an overlapping sequence at the site of mutation and were subsequently used to prime each other in an extension reaction of one cycle, followed by the addition of universal primers to amplify the full gene. Following digestion with *Eco*RI and *Bam*HI, the purified 1.5 kb product was ligated into the pVL1392 expression vector (Pharmingen) and propagated in *E. coli*. Each mutant-containing plasmid was sequenced using primers NA400' (5'-CAA GTG TTA TCA ATT TGC-3') and NA782' (5'-CTA TTC ATT GAA GAG GGG-3').

Next, the mutant plasmids were cotransfected, isolated, and amplified as described for the wild type.<sup>32</sup> High-titer virus stocks were produced from single isolates in three passages. The recombinant baculovirus DNA was isolated from high-titer virus stocks according to established procedures<sup>33</sup> and sequenced using primers NA400', NA782', BV1' (5'-TTT ACT GTT TTC GTA ACA GTT TTG-3'), and BV2' (5'-CAA CAA CGC ACA GAA TCT AGC-3'). Recombinant viral DNA sequence analysis of the full sialidase gene confirmed that the recombinant baculovirus stocks did indeed contain the correct substitutions for the five different mutations.

**Influenza Viral Sialidase Mutant Expression.** Two separate small-scale expressions of the five mutants were performed in *Trichoplusia ni* insect cells using 60 mm plates as well as 100 mL spin cultures. After 65 h at 27 °C and 100 rpm, crude supernatants were analyzed. Crude culture supernatant samples from the small-scale trial expressions of the five mutants were analyzed by Western blotting and activity assays. On the basis of the Western blot data, mutants D151N and E277D were expressed and purified on a large scale (1.0–2.4 L) for characterization. Although the small-scale production of the D151A mutant gave no detectable protein by Western blot analysis, it was also expressed on a 2 L scale to determine whether any mutant sialidase was present, even at extremely low levels. Comparison of concentrated D151A expression samples with the wild type, D151N, and E277D revealed that no D151A mutant was present. A total of six different virus isolates were analyzed by Western blotting to check for a positive sign of expression, though nothing was observed for D151A, D151G, or E277Q.

**Polyclonal Antibodies.** A polyclonal antibody was raised against a peptide from a known antigenic loop region that is not close to the catalytic site of the influenza sialidase.<sup>34</sup> Peptide NA324 (DTPRNDRRSSNSNC) conjugated to the carrier protein keyhole limpet hemocyanin was used to immunize two rabbits (Genemed Synthesis, Inc.). Immunoblotting<sup>35</sup> and enzyme-linked immunosorbent assay (ELISA) procedures were performed using a primary antibody dilution of 1:1000. The antiserum raised against peptide NA324 was tested by ELISA and Western blotting for response to the peptide itself as well as crude and pure wild-type A/Tokyo/3/67 sialidase under denaturing conditions (data not shown). Antisera from both rabbits solicit a specific response from the whole recombinant A/Tokyo/3/67 sialidase with minimal background.

**Purification of Influenza Sialidase Mutants D151N and E277D.** The purification of E277D and D151N followed the same protocol that was used for the wild-type enzyme.<sup>32</sup> Purification was monitored by both sialidase activity assay and

immunological techniques. The total protein concentrations of the pure stocks determined by the Micro BCA assay were within 3% of the results of a Bradford assay, using ultrapure BSA as the standard. Overall yields were 105 and 57 µg of E277D and D151N, respectively, per liter of culture.

**Enzyme Kinetics of *M. viridifaciens*.** The progress of the reactions was continuously monitored for 10 min using either a Cary 3E spectrophotometer (UV-vis) or a Cary Eclipse fluorimeter equipped with a Peltier temperature controller. Michaelis–Menten parameters were determined from a minimum of seven initial rate measurements within a substrate concentration range of at least  $K_m/4$  to  $4K_m$ . The rate versus substrate concentration data were fit to a standard Michaelis–Menten equation using Prism 4.0. The effect of leaving group ability was monitored at 25 °C in 100 mM acetate buffer (pH 5.25) using a series of aryl *N*-acetylneuraminides and 3'-MUG- $\alpha$ Neu5Ac. The reactions of aryl substrates were monitored using UV-vis spectroscopy at various wavelengths (see Tables S6 and S7 of the Supporting Information), and the reactions of MU- $\alpha$ Neu5Ac and 3'-MUG- $\alpha$ Neu5Ac were monitored as reported previously.<sup>24</sup> To test for buffer catalysis, we monitored the E260C-catalyzed hydrolysis of MU- $\alpha$ Neu5Ac (over a substrate concentration range of 0.5–9.0 µM) in both acetate and homopipes buffers (100 mM buffer;  $I = 0.1$ , KCl) at pH 5.25.

For the case of the E260D mutant, <sup>1</sup>H NMR spectroscopy was used to construct a relative Brønsted plot for  $k_{cat}/K_m$ . Specifically, MU- $\alpha$ Neu5Ac and an aryl *N*-acetylneuraminide (approximately 0.5 mg of each substrate) were combined in sodium formate buffer in D<sub>2</sub>O (600 µL, 100 mM, pD 5.25). Following the addition of enzyme, the relative amounts of each substrate remaining were monitored as a function of time. The ratio of substrates remaining versus the fraction of reaction of MU- $\alpha$ Neu5Ac was fit to eq 1

$$Y = (1 - X)^{(1/k_{rel})-1} \quad (1)$$

where  $X$  is the fraction of the reaction of MU- $\alpha$ Neu5Ac, which was calculated using the C–H signal from the sodium formate buffer as an internal standard, and  $Y$  is the ratio of the two remaining substrate concentrations.

The Brønsted plot on  $k_{cat}$  for the E260D mutant was generated by monitoring the hydrolysis reactions at a single high substrate concentration. For the E260C mutant at pH 7.9 (100 mM MOPS-NaOH at 25 °C),  $k_{cat}$  values were measured with MU- $\alpha$ Neu5Ac and 3'-MUG- $\alpha$ Neu5Ac as substrates. The auxiliary enzyme used to hydrolyze the galactoside intermediate released from 3'-MUG- $\alpha$ Neu5Ac was *E. coli*  $\beta$ -galactosidase.

**pH–Rate Profile.** To determine the effect of pH on catalysis, we took kinetic measurements using MU- $\alpha$ Neu5Ac as the substrate over a pH range of 3.78–7.90. The following buffers (50 mM,  $I = 0.1$ , KCl) were used: NaOAc-HOAc (pH range of 3.78–5.00), 2-(*N*-morpholino)ethanesulfonic acid (MES-NaOH) (pH range of 5.62–6.50), and 3-(*N*-morpholino)propanesulfonic acid (MOPS-NaOH) (pH range of 7.20–7.90). Fluorescence intensity calibration plots were generated for each of the 11 buffers used in these experiments.

**Solvent Kinetic Isotope Effect.** Buffers were prepared via addition of equivalent concentrations of HCl or DCl (12 mM) to generate buffers with identical AcOL:AcO<sup>−</sup> concentration ratios of 12:38 ( $L = H$  or  $D$ ) with a total buffer concentration of 50 mM in H<sub>2</sub>O or D<sub>2</sub>O, respectively.<sup>36</sup> Reaction rates were determined at varying deuterium fractions by mixing the appropriate ratios of the H<sub>2</sub>O and D<sub>2</sub>O buffers. Substrate



concentrations ( $10.75K_m$ ) in  $H_2O$  and  $D_2O$  buffers were adjusted to a <1% difference using UV–vis spectroscopy. To ensure that the enzyme concentrations do not impact the observed rates, the same enzyme stock solution in  $H_2O$  was added to each reaction mixture. After dilution, the total  $H_2O$  content from the enzyme solution was less than 2% of the total volume.

**Enzyme Kinetics of the Influenza Virus.** The pure mutant sialidases were characterized in comparison to the wild-type enzyme with PNP- $\alpha$ Neu5Ac as the substrate.<sup>32</sup> To achieve E277D mutant-catalyzed hydrolysis rates that were significant compared to the rate of the background reaction, it was necessary to measure kinetic parameters in a pH 8.0 buffer (50 mM HEPES, 0.1 mM  $CaCl_2$ , 0.32 mM  $MgCl_2$ , and 60 mM NaCl) at 25 °C. Kinetic parameters with an abridged natural substrate,  $\alpha$ -(2→3)sialyllactose [3'-Lac- $\alpha$ Neu5Ac (V-laboratories)], were determined by assaying for the liberated sialic acid product (Sialic-Q Quantitation Kit, Sigma-Aldrich). The binding constant of 3'-Lac- $\alpha$ Neu5Ac with E277D was measured using a competitive binding assay. Specifically, the  $IC_{50}$  of 3'-Lac- $\alpha$ Neu5Ac with E277D was measured using MU- $\alpha$ Neu5Ac under conditions where the value for  $IC_{50}$  is within 10% of that for  $K_i$ .<sup>37</sup>

## RESULTS AND DISCUSSION

**M. viridifaciens Sialidase Mutants.** To understand how the strictly conserved glutamic acid residue affects the catalytic rate of sialidases, we cloned and expressed four different E260 mutants (E260A, E260C, E260D, E260H) of the *M. viridifaciens* enzyme in *E. coli*. Interestingly, preliminary kinetic data showed that the relative activities of the crude E260 mutants for catalyzing the hydrolysis of 4-methylumbelliferyl  $\alpha$ -D-sialoside (MU- $\alpha$ Neu5Ac) at pH 5.25, adjusted for their comparative SDS–PAGE band intensities, were in following order: wild type > cysteine > aspartic acid  $\approx$  histidine > alanine. Accordingly, detailed kinetic experiments were performed using purified stocks of the two most active mutants, E260C and E260D, which were expressed and purified separately using fresh resin to prevent any possible contamination with other mutants or wild-type enzyme. The use of NMR spectroscopy, as previously reported,<sup>18</sup> showed that both enzymes are retaining sialidases (Figures S1 and S2 of the Supporting Information) and that the gross mechanism of action has not changed, in contrast to those of some active site tyrosine mutants.<sup>18,21</sup>

Given in Table S1 (Supporting Information) are the derived Michaelis–Menten parameters for the E260C mutant sialidase-catalyzed hydrolysis of substrates 1–6. For the E260D mutant enzyme, it was impossible to measure accurate  $k_{cat}/K_m$  values for substrates in which the leaving group was not fluorescent because of the low apparent  $K_m$  values associated with this mutant sialidase. Therefore,  $k_{cat}$  values were measured separately at high substrate concentrations (Table S2 of the Supporting Information), and  $k_{cat}/K_m$  values were measured relative to that for MU- $\alpha$ Neu5Ac by comparing the proportionate rates of reaction in an NMR spectrometer (Table S3 of the Supporting Information; see Materials and Methods for full details). The derived Brønsted  $\beta_{lg}$  values on  $k_{cat}$  for the E260C and E260D mutant sialidases are  $-0.06 \pm 0.04$  and  $-0.02 \pm 0.06$ , respectively (Figure 2), and the corresponding  $\beta_{lg}$  values on  $k_{cat}/K_m$  are  $-0.20 \pm 0.04$  and  $-0.54 \pm 0.07$ , respectively (Figure 3). Also shown in Figures 2 and 3 are the kinetic data for the wild-type *M. viridifaciens* sialidase,<sup>18,25</sup> where the

reported  $\beta_{lg}$  values for  $k_{cat}$  and  $k_{cat}/K_m$  are  $0.02 \pm 0.03$  and  $-0.30 \pm 0.04$ , respectively.<sup>18</sup>

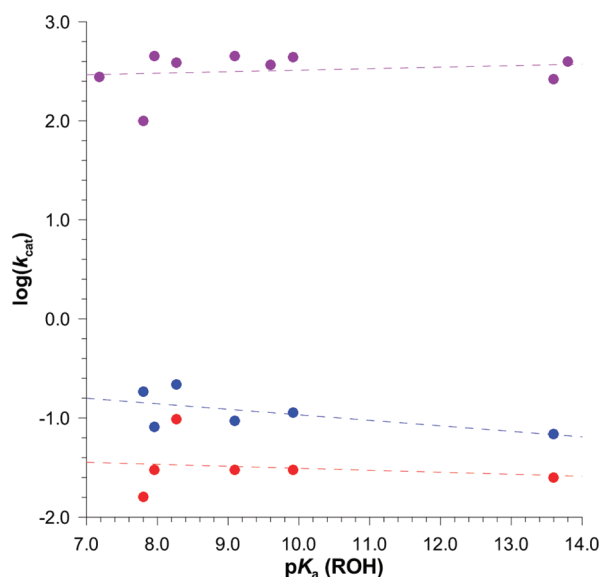


**Figure 2.** Effect of leaving group ability on  $k_{cat}$  for the wild type (mauve circles), E260C (blue circles), and E260D (red circles) at 25 °C and pH 5.25. Leaving group ability is represented as  $pK_a$  ( $BH^+$ ) as follows: 4-methylumbelliferone (7.80), 4-cyanophenol (7.96), 3-nitrophenol (8.27), 3-chlorophenol (9.09), phenol (9.92), and 4-methylumbelliferyl galactoside [3-OH (13.6)]. Data for the wild-type enzyme were taken from refs 18 and 25. The dotted lines are the best linear fits to the data.

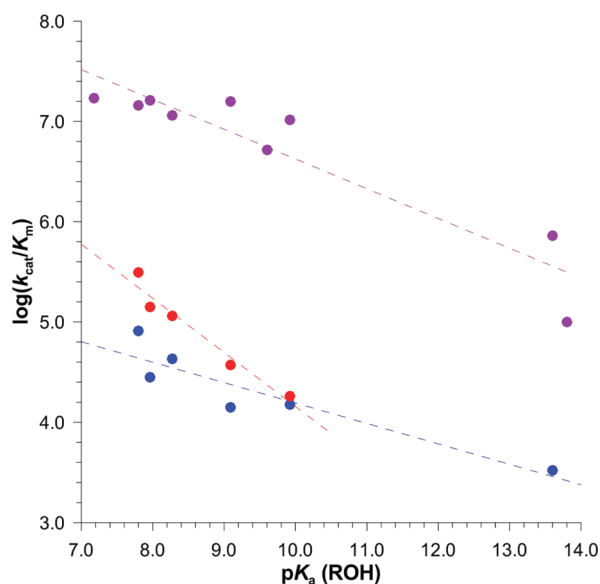


**Figure 3.** Effect of leaving group ability on  $k_{cat}/K_m$  for the wild type (mauve circles), E260C (blue circles), and E260D (red circles) at 25 °C and pH 5.25. Leaving group ability is represented as  $pK_a$  ( $BH^+$ ) as follows: 4-methylumbelliferone (7.80), 4-cyanophenol (7.96), 3-nitrophenol (8.27), 3-chlorophenol (9.09), phenol (9.92), and 4-methylumbelliferyl galactoside [3-OH (13.6)]. Data for the wild-type enzyme were taken from refs 18 and 25. The dotted lines are the best linear fits to the data.

The mutation of the catalytic glutamate residue to a cysteine results in an enzyme in which the  $\beta_{lg}$  values for both kinetic

parameters,  $k_{\text{cat}}$  and  $k_{\text{cat}}/K_{\text{m}}$ , are essentially unchanged from those of the wild-type *M. viridifaciens* sialidase. As such, it is likely that the kinetically significant steps for the wild-type and E260C mutant enzymes are similar with the rate constant decrease between these sialidases being a direct measurement of the change in transition state (TS) stabilization caused by the glutamate to cysteine mutation. That is,  $k_{\text{cat}}/K_{\text{m}}$  reports all steps up to and including the first irreversible step, i.e., glycosylation, which on the basis of the Brønsted  $\beta_{\text{lg}}$  value for the *M. viridifaciens* enzyme involves a kinetically significant glycosylation reaction, while the  $k_{\text{cat}}$  TS involves deglycosylation.<sup>38</sup> On the other hand, changing the side chain of the glutamic acid to the shorter aspartic acid residue has little effect on the  $\beta_{\text{lg}}$  value for  $k_{\text{cat}}$ , once again consistent with deglycosylation being the overall rate-limiting step as it is for the wild-type enzyme,<sup>38</sup> whereas the second-order rate constant,  $k_{\text{cat}}/K_{\text{m}}$ , shows a significant change in calculated  $\beta_{\text{lg}}$  values from  $-0.30$  (wild type) to  $-0.54$  (E260D).<sup>18</sup> These observations indicate that catalysis for the glycosylation reaction is more severely compromised for the E260D mutant sialidase than it is for the E260C enzyme.

To investigate how the catalytic activity for both of the *M. viridifaciens* glutamate mutant enzymes varied with pH, full Michaelis–Menten curves were measured for the hydrolysis of MU- $\alpha$ Neu5Ac at multiple pH values. Shown in Figure 4 are the

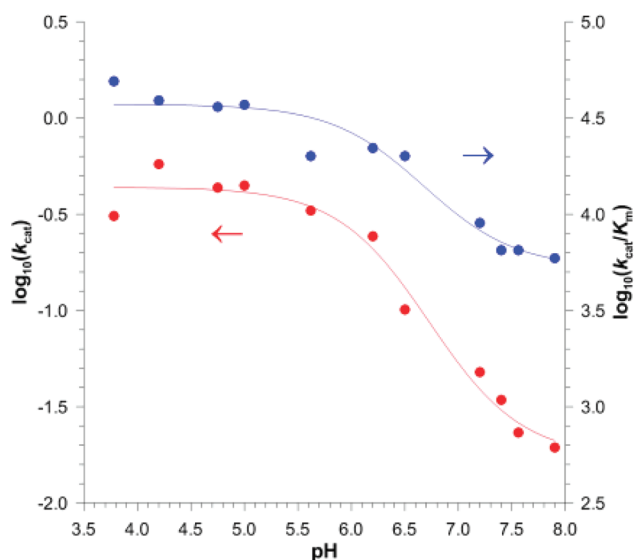


**Figure 4.** Effect of pH on  $k_{\text{cat}}$  (red circles) and  $k_{\text{cat}}/K_{\text{m}}$  (blue circles) for the E260C mutant sialidase-catalyzed hydrolysis of MU- $\alpha$ Neu5Ac at 25 °C. The solid lines are the best nonlinear fits to a standard titration curve for the data.

kinetic data for the hydrolysis of MU- $\alpha$ Neu5Ac catalyzed by the E260C mutant enzyme (data listed in Table S4 of the Supporting Information).

We showed that the observed catalytic activity of the E260C mutant enzyme at low pH values did not result from “chemical rescue” by the carboxylic acid buffer, an occurrence that has been reported in the literature for standard retaining glycosidases,<sup>39,40</sup> as we measured identical reaction rates in acetate and homopipes buffers over a substrate concentration range that spanned  $K_{\text{m}}$  (Table S1 of the Supporting Information).

Of note, for both kinetic parameters,  $k_{\text{cat}}$  and  $k_{\text{cat}}/K_{\text{m}}$ , the E260C mutant enzyme is more active at low pH values (Figure 4), with the inflection point for both profiles occurring at the same pH value ( $k_{\text{cat}} = 6.73 \pm 0.13$ , and  $k_{\text{cat}}/K_{\text{m}} = 6.68 \pm 0.20$ ). To check whether the notable decrease in activity at high pH values is caused by a change in the rate-determining step,  $k_{\text{cat}}$  values were measured for two substrates at the extrema of the Brønsted plot. Specifically, at pH 7.9 (100 mM MOPS-NaOH at 25 °C), the measured  $k_{\text{cat}}$  values for the E260C mutant *M. viridifaciens* sialidase-catalyzed hydrolysis of MU- $\alpha$ Neu5Ac [ $1$ ;  $\text{p}K_{\text{a}}(\text{ROH}) = 7.8$ ] and 4-methylumbelliferyl  $\alpha$ -D-sialosyl-(2→3)- $\beta$ -D-galactopyranoside [ $6$ , 3’MUG- $\alpha$ Neu5Ac;  $\text{p}K_{\text{a}}(\text{ROH}) = 13.6$ ] are  $0.00823 \pm 0.0055$  and  $0.00786 \pm 0.0032 \text{ s}^{-1}$ , respectively. We therefore conclude that deglycosylation is the kinetically significant mechanistic step for  $k_{\text{cat}}$  over the whole studied pH range.

The solvent deuterium kinetic isotope effect (SDKIE) on  $k_{\text{cat}}$  for the E260C mutant ( $k_{\text{H}_2\text{O}}/k_{\text{D}_2\text{O}}$ ) was measured to be  $2.31 \pm 0.09$  by maintaining identical ratios of the two buffer components in  $\text{H}_2\text{O}$  and  $\text{D}_2\text{O}$ , as advocated by Schowen.<sup>36</sup> The magnitude of the SDKIE is consistent with proton transfer occurring at the TS for deglycosylation. Of note, it is clear that deglycosylation of the wild-type enzyme involves weak general acid catalysis from the glutamic acid residue and no general base catalysis<sup>38</sup> and that hydrolysis of phenyl  $\beta$ -D-sialoside bound to the Y370G *M. viridifaciens* mutant sialidase, a situation in which the Michaelis complex mimics the tyrosinyl–enzyme intermediate, occurs with no general base catalysis.<sup>27</sup> Consequently, the origin of the observed SDKIE for the E260C mutant enzyme is likely general acid-catalyzed cleavage of the tyrosinyl–sialoside bond. We therefore measured a proton inventory (Figure 5)<sup>41</sup> on  $k_{\text{cat}}$  for the E260C mutant–

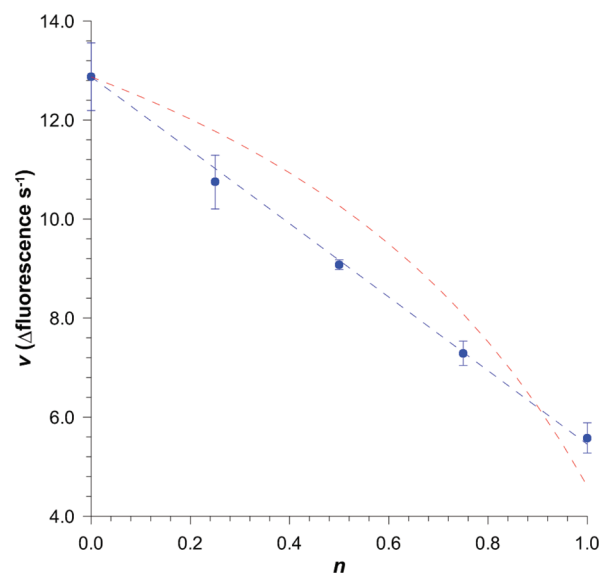


**Figure 5.** Plot of  $k_n$  for the E260C mutant *M. viridifaciens* sialidase-catalyzed hydrolysis of MU- $\alpha$ Neu5Ac as a function of  $n$  (mole fraction of deuterium in the solvent) at 25 °C. The error bars represent two standard deviations; the dotted blue line is the best linear fit to the data, and the dotted red line is the best fit to a single-proton transfer model involving an S–H/D bond.

catalyzed hydrolysis of MU- $\alpha$ Neu5Ac to probe the origin of this effect.

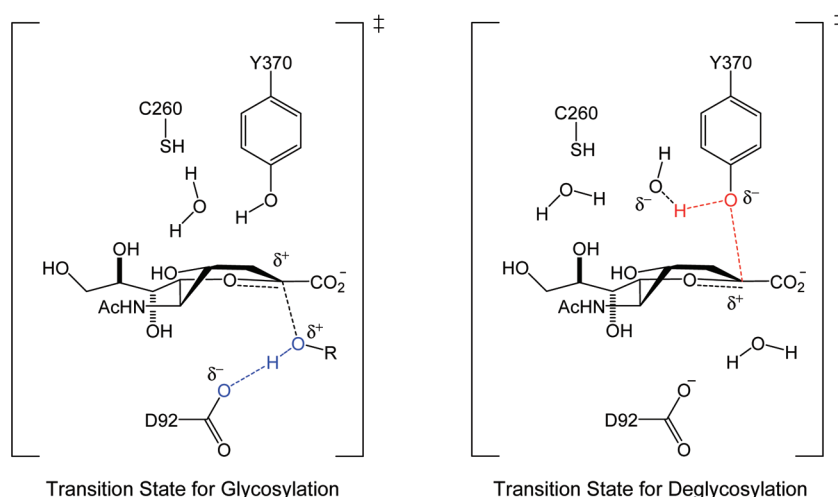


**Figure 6.** Postulated transition state structures for glycosylation and deglycosylation of the *M. viridifaciens* E260C mutant sialidase-catalyzed hydrolysis of MU- $\alpha$ Neu5Ac.

Shown in eq 2 is the Gross–Butler equation that describes the functional relationship between the rate constant  $k_n$ , where  $n$  is the fraction of deuterium in  $\text{H}_2\text{O}/\text{D}_2\text{O}$  mixtures, and  $\varphi_i$  and  $\varphi_j$ , which are the fractionation factors for protons in reactant and transition state sites, respectively.

$$k_n = k_0 \frac{\prod_j^{\text{TS}} (1 - n - n\varphi_j)}{\prod_i^{\text{RS}} (1 - n - n\varphi_i)} \quad (2)$$

The linear proton inventory allows us to rule out a single proton “in flight” from the cysteine sulfur atom to the tyrosinyl-bound intermediate as the reactant site fractionation factor for an S–H bond ( $\varphi_1 = 0.46$ ) would result in a concave down appearance in the plot (the best fit to this model, red line, is shown in Figure 5).<sup>41</sup> However, as is common with the proton inventory technique, the observed rate constants are consistent with more than one model. In this case, it is compatible with either (i) a single proton in flight at the TS for deglycosylation, which does not involve the cysteine sulfur atom,<sup>36,42</sup> or (ii) two protons in flight, one of which is on the thiol.<sup>36,41,42</sup> In the absence of further evidence, we hypothesize that general acid catalysis of tyrosine departure involves a bound water molecule, which is located in the void created by the E260C mutation (i.e., not involving the cysteine). Although we have no further kinetic or structural evidence for a bound water molecule in the E260C mutant, we note that the change in molar volume upon replacement of a glutamic acid with a cysteine residue is  $\sim 16 \text{ cm}^3/\text{mol}$ ,<sup>43</sup> a value that is similar to that of a single water molecule ( $18 \text{ cm}^3/\text{mol}$ ). Regardless of whether a water molecule binds in this cavity, it is clear that tyrosine remains the catalytic nucleophile in these mutant sialidases.

Thus, we conclude that the pH dependence of the E260C mutant sialidase activity mirrors the protonation state of the catalytic aspartic acid residue, that is, D92 in the *M. viridifaciens* enzyme (Figure 1). Specifically, we suggest that removal of the general base component of the nucleophilic dyad [E260 and Y370 (Figure 1)] necessitates a greater contribution to catalysis by the aspartic acid residue located on the opposite face of the active site, with the result that the E260C mutant is more active when this residue is protonated. With respect to glycosylation, TS charge development on the carbohydrate moiety is surely

facilitated by polarization of the tyrosine nucleophile by the adjacent glutamate, an interaction that is absent in the E260C mutant (Figure 6). Indeed, a recent theoretical paper describes the thermodynamic profile for the transfer of hydrogen between the active site glutamate and tyrosine residues in the *trans*-sialidase from *Trypanosoma cruzi*.<sup>44</sup> Specifically, the proton transfer becomes less endergonic upon substrate binding, with a resultant increase in the negative charge on the tyrosinyl oxygen atom,<sup>44</sup> which we suggest stabilizes the formation of an oxacarbenium ion-like TS. Moreover, the deglycosylation TS involves general acid catalysis from a water molecule with the ultimate origin of the proton likely being a remote residue, such as Asp259, via a chain of bound water molecules (Figure 6).

In contrast to that of the E260C mutant sialidase, the pH–rate profiles for both  $k_{\text{cat}}$  and  $k_{\text{cat}}/K_m$  with the E260D mutant enzyme apparently show bell-shaped profiles, which suggest the involvement of two important ionizations (Figure 7; data listed in Table S5 of the Supporting Information). However, because of the smaller quantities of the E260D mutant enzyme available, we were unable to measure kinetic data over a larger pH range than that from pH 3.6 to 6.2 (Figure 7), and the maximal changes in  $k_{\text{cat}}$  and  $k_{\text{cat}}/K_m$  values over this narrow pH range are 6- and 3-fold, respectively. Notwithstanding the small changes, we speculate that the origins for these effects are that (i) at low pH the newly installed Asp-260 is protonated and (ii) at high pH values the conserved general acid Asp-92 is deprotonated, and that both of these proton transfer events result in a less active mutant enzyme.

**Influenza Viral Sialidase Mutants.** The influenza viral mutant proteins were expressed in *T. ni* insect cells, and via a crude assay, the E277D but not the E277Q mutant hydrolyzed the substrate MU- $\alpha$ Neu5Ac. Figure 8 shows a Western blot for crude expression samples of all five (two Glu-277 and three Asp-151) mutants in comparison with the wild-type expression and negative control cultures.

The samples shown on the Western blot contain only protein, both virus-bound and free in the supernatant after prolonged expression (see Materials and Methods). As a result, there are multiple forms of the sialidase present, presumably resulting from different glycoforms and proteolytic cleavage sites. For large-scale expressions, the cultures were harvested

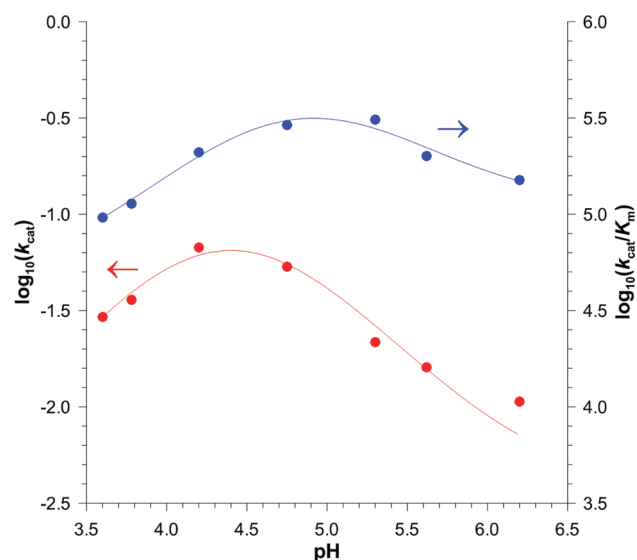


**Figure 7.** Effect of pH on  $k_{\text{cat}}$  (red circles) and  $k_{\text{cat}}/K_m$  (blue circles) for the E260D mutant sialidase-catalyzed hydrolysis of MU- $\alpha$ Neu5Ac at 25 °C. The solid lines are the best nonlinear fits to a standard “bell-shaped” pH–activity curve for the data.

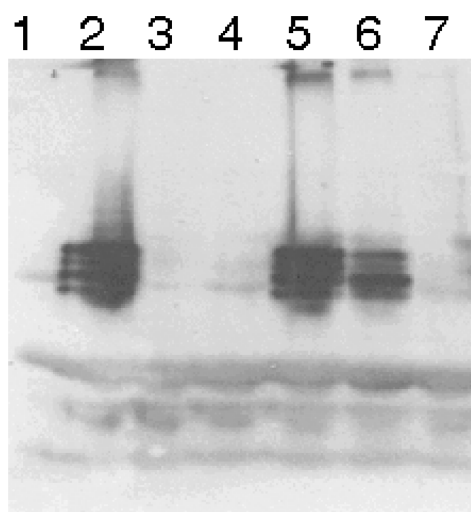


**Figure 8.** Western blot analysis of crude expression supernatant samples (bands represent virus-associated and free forms). Each lane contains 100  $\mu\text{L}$  of culture supernatant harvested 65 h postinfection: lane 1, negative control from cells infected with baculovirus but no neuraminidase gene; lane 2, expression of the recombinant wild-type influenza neuraminidase; lane 3, D151A; lane 4, D151G; lane 5, D151N; lane 6, E277D; lane 7, E277Q.

much earlier and a single species of sialidase was isolated by cleavage of the protease from the surface of the baculovirus particles.

**Influenza Sialidase E277 Mutants.** The E277D substitution yielded an active protein, while the E277Q substitution did not. Because of the low activity of E277D, kinetic experiments were performed at 25 °C and pH 8.0 to increase the sensitivity of the assay. Table 1 lists the measured catalytic constants for the wild-type and E277D sialidases. Although no turnover was detected for the abridged natural substrate (3'-Lac- $\alpha$ Neu5Ac) in the presence of E277D, the substrate binds to both the mutant and wild type with comparable affinities ( $K_d = 2.2$  and 0.5 mM, respectively).

**Influenza Sialidase D151 Mutants.** Unfortunately, only one aspartate mutant gave detectable quantities of protein (D151N), and this enzyme gained hydrolytic activity over time. Over the course of purification, extreme care was taken to avoid cross contamination (i.e., isolated storage, new resin, disposable vessels, and two independent purifications). During kinetic runs, the wild-type and D151N stocks were never open at the same time. Therefore, direct cross contamination with the wild type is unlikely. An explanation for the observed effect is that a spontaneous deamination of the encoded asparagine occurs to generate an aspartate-containing enzyme, i.e., reversion to the wild-type phenotype. Other researchers who have studied analogous mutations in glycosidases have reported similar observations.<sup>45,46</sup>

**Contributions to Catalysis.** Previous studies that involve mutagenesis of the strictly conserved active site glutamic acid residue focused mainly on whether this residue was important for catalysis. First, the same mutation (E277D) in the influenza enzyme, which was expressed in a different system (vaccinia virus), resulted in an enzyme that was inactive toward natural substrates.<sup>12</sup> Unfortunately, Lentz et al. could not obtain pure enzyme to characterize any of their mutants thoroughly.<sup>12,47</sup> Second, various substitutions were made to the small sialidase from *Clostridium perfringens*, and the reduced activity of these E230 mutants against activated substrates led these authors to conclude that this residue is important for catalysis.<sup>48,49</sup> Third, a serine mutant of E225 in the human enzyme NEU3 reduced enzyme activity, measured using the activated substrate MU- $\alpha$ Neu5Ac, to 0.3% of that of wild-type sialidase.<sup>50</sup>

Initial attempts to probe the activity of this strictly conserved glutamic acid residue centered on the clinically important sialidase from influenza virus type A. However, the low yield of protein and the poor catalytic activity of the E277D mutant enzyme precluded a detailed mechanistic study. Thus, the activity of this mutant protein was measured with an activated substrate (pNP- $\alpha$ Neu5Ac) and an abridged natural substrate (3'-Lac- $\alpha$ Neu5Ac). The decreases in catalytic efficiency ( $k_{\text{cat}}/K_m$ ) upon mutation of E277 to an aspartate residue for the influenza enzyme result in free energy increases for hydrolysis of pNP- $\alpha$ Neu5Ac and 3'-Lac- $\alpha$ Neu5Ac (pH 8.0 and 25 °C) of 18.0 and >26.1 kJ/mol, respectively.

**Table 1.** Michaelis–Menten Kinetic Parameters for the Recombinant Influenza A/Tokyo/3/67 Wild-Type and E277D Mutant Sialidases with Various Substrates

enzyme	pNP- $\alpha$ Neu5Ac		3'-Lac- $\alpha$ Neu5Ac	
	$k_{\text{cat}}$ ( $\text{s}^{-1}$ )	$k_{\text{cat}}/K_m$ ( $\text{M}^{-1} \text{s}^{-1}$ )	$k_{\text{cat}}$ ( $\text{s}^{-1}$ )	$k_{\text{cat}}/K_m$ ( $\text{M}^{-1} \text{s}^{-1}$ )
WT <sup>a</sup>	$26.2 \pm 1.3$	$(2.8 \pm 0.5) \times 10^5$	$10.7 \pm 0.6$	$(9.8 \pm 2.2) \times 10^3$
WT <sup>b</sup>	$1.82 \pm 0.05$	$(1.8 \pm 0.2) \times 10^4$	$4.5 \pm 0.2$	$(9.6 \pm 2.1) \times 10^3$
E277D <sup>b</sup>	$0.012 \pm 0.002$	$13 \pm 5$	$<5.7 \times 10^{-4c}$	$<0.26^c$

<sup>a</sup>pH 6.0 and 37 °C data from ref 32. <sup>b</sup>pH 8.0 and 25 °C. <sup>c</sup>These values represent upper limits as no activity was detected.



A comment about why the glutamic acid residue is strictly conserved in sialidases when, at least for the *M. viridifaciens* enzyme, replacement gives active enzymes is warranted. We note that sialyl-based ketal centers are intrinsically  $\sim 10^5$  times more reactive than normal glycopyranosides,<sup>18</sup> and as a result of the greater inherent reactivity of ketal-based *N*-acetylneuraminides, the catalytic rate enhancement provided by any of the three active site residues [Y370, E260, and D92 (Figure 1)] is smaller than that reported for the two catalytic residues that operate on the less reactive acetal-based glycopyranosyl-retaining hydrolases.

Unquestionably, activated substrates, which are generally used because of the associated large change in either fluorescence or absorbance upon their hydrolysis, give rise to misleading conclusions with respect to the catalytic rate enhancement endowed by a particular active site residue. It is critical to recognize that unactivated substrates (3'-Lac- $\alpha$ Neu5Ac or 3'-MUG- $\alpha$ Neu5Ac) require a greater degree of catalysis to react than do substrates bearing activated leaving groups. Similar conclusions have been made on the basis of kinetic analyses of the catalytic tyrosine<sup>18,20</sup> and aspartic acid<sup>19</sup> mutants of the sialidase from *M. viridifaciens*.

## CONCLUSIONS

In summary, we have performed mechanistic investigations of active site mutants of the conserved glutamic acid residue, which is a member of the catalytic triad, using the sialidases from *M. viridifaciens* and influenza A (N2). In the case of the *M. viridifaciens* enzyme, we conclude that the results of this study when combined with the published reports concerning mutation of the other two catalytic residues<sup>18,19,21,29</sup> show that removal of any one of these strictly conserved triad residues (Asp-92, Glu-260, and Tyr-370) results in catalytically competent mutant enzymes in which the catalytic role of the mutated residue is partially offset by the two remaining residues. These findings provide detailed insight into an unusual glycosidase mechanism and suggest several protein engineering applications of these highly versatile and robust catalysts.

## ASSOCIATED CONTENT

### Supporting Information

Figures S1 and S2 and Tables S1–S7. This material is available free of charge via the Internet at <http://pubs.acs.org>.

## AUTHOR INFORMATION

### Corresponding Author

\*E-mail: [bennet@sfu.ca](mailto:bennet@sfu.ca). Telephone: (778) 782-8814. Fax: (778) 782-3765.

### Present Addresses

<sup>§</sup>Northern Catalyst Scientific Consulting, 76 North Star Dr., Whitehorse, Yukon Y1A 0A3, Canada.

<sup>||</sup>Douglas College, P.O. Box 2503, New Westminster, British Columbia V3L 5B2, Canada.

### Funding

Funded by the Natural Science and Engineering Research Council of Canada. J.N.W. thanks BC Science Council for receipt of a GREAT scholarship

## ACKNOWLEDGMENTS

J.N.W. thanks Twinstrand Therapeutics for access to their cell culture facility. Thanks to Dr. Gillian Air for the clone of the

wild-type A/Tokyo/3/67 sialidase gene and to Drs. Wakarchuk and Gilbert for the 2,3-sialyltransferase used in the synthesis of 3'-MUG- $\alpha$ Neu5Ac.

## ABBREVIATIONS

homopipes, homopiperazine-*N,N'*-bis(2-ethanesulfonic acid); 3'-Lac- $\alpha$ Neu5Ac,  $\alpha$ -(2 $\rightarrow$ 3)sialyllactose; MES, 2-(*N*-morpholino)ethanesulfonic acid; MOPS, 3-(*N*-morpholino)propanesulfonic acid; MU- $\alpha$ Neu5Ac, 4-methylumbelliferyl  $\alpha$ -D-*N*-acetylneuraminide; 3'-MUG- $\alpha$ Neu5Ac, 4-methylumbelliferyl  $\alpha$ -D-sialosyl-(2 $\rightarrow$ 3)- $\beta$ -D-galactopyranoside; MvNA, *M. viridifaciens* neuraminidase; Neu5Ac, *N*-acetylneuraminic acid; PNP- $\alpha$ Neu5Ac, *p*-nitrophenyl  $\alpha$ -D-*N*-acetylneuraminide.

## REFERENCES

- (1) Davies, G., Sinnott, M. L., and Withers, S. G. (1998) Glycosyl Transfer. In *Comprehensive Biological Catalysis* (Sinnott, M. L., Ed.) 1st ed., pp 119–209, Academic Press, San Diego.
- (2) Wilson, J. C., Angus, D. I., and von Itzstein, M. (1995) <sup>1</sup>H NMR evidence that *Salmonella typhimurium* sialidase hydrolyzes sialosides with overall retention of configuration. *J. Am. Chem. Soc.* 117, 4214–4217.
- (3) Saito, M., and Yu, R. K. (1995) Biochemistry and function of sialidases. In *Biology of the Sialic Acids* (Rosenberg, A., Ed.) pp 261–313, Plenum Press, New York.
- (4) Schauer, R., Kelm, S., Reuter, G., and Roggentin, P. (1995) Biochemistry and role of sialic acids. In *Biology of the Sialic Acids* (Rosenberg, A., Ed.) pp 7–67, Plenum Press, New York.
- (5) Henrissat, B. (1991) A classification of glycosyl hydrolases based on amino acid sequence similarities. *Biochem. J.* 280, 309–316.
- (6) Henrissat, B., and Bairoch, A. (1993) New families in the classification of glycosyl hydrolases based on amino acid sequence similarities. *Biochem. J.* 293, 781–788.
- (7) Henrissat, B., and Bairoch, A. (1996) Updating the sequence-based classification of glycosyl hydrolases. *Biochem. J.* 316, 695–696.
- (8) Palese, P., Tobita, K., Ueda, M., and Compans, R. W. (1974) Characterization of temperature sensitive influenza virus mutants defective in neuraminidase. *Virology* 61, 397–410.
- (9) Aisaka, K., Igarashi, A., and Uwajima, N. (1991) Purification, crystallization, and characterization of neuraminidase from *Micromonospora viridifaciens*. *Agric. Biol. Chem.* 55, 997–1004.
- (10) Sakurada, K., Ohta, T., and Hasegawa, M. (1992) Cloning, expression, and characterization of the *Micromonospora viridifaciens* neuraminidase gene in *Streptomyces lividans*. *J. Bacteriol.* 174, 6896–6903.
- (11) Vimr, E. R. (1994) Microbial sialidases: Does bigger always mean better? *Trends Microbiol.* 2, 271–277.
- (12) Lentz, M. R., Webster, R. G., and Air, G. M. (1987) Site-directed mutation of the active site of influenza neuraminidase and implications for the catalytic mechanism. *Biochemistry* 26, 5351–5358.
- (13) Chong, A. K. J., Pegg, M. S., Taylor, N. R., and von Itzstein, M. (1992) Evidence for a sialosyl cation transition-state complex in the reactivity of sialidase from influenza virus. *Eur. J. Biochem.* 207, 335–343.
- (14) Ghatge, A. A., and Air, G. M. (1998) Site-directed mutagenesis of catalytic residues of influenza virus neuraminidase as an aid to drug design. *Eur. J. Biochem.* 58, 320–331.
- (15) Guo, X., Laver, W. G., Vimr, E., and Sinnott, M. L. (1994) Catalysis by two sialidases with the same protein fold but different stereochemical courses: A mechanistic comparison of the enzymes from influenza A virus and *Salmonella typhimurium*. *J. Am. Chem. Soc.* 116, 5572–5578.
- (16) Varghese, J. N., and Colman, P. M. (1991) Three-dimensional structure of the neuraminidase of influenza virus A/Tokyo/3/67 at 2.2 Å resolution. *J. Mol. Biol.* 221, 473–486.
- (17) Varghese, J. N., McKimm-Breschkin, J. L., Caldwell, J. B., Kortt, A. A., and Colman, P. M. (1992) The structure of the complex

between influenza virus neuraminidase and sialic acid, the viral receptor. *Proteins: Struct., Funct., Genet.* 14, 327–332.

(18) Watson, J. N., Dookhun, V., Borgford, T. J., and Bennet, A. J. (2003) Mutagenesis of the conserved active-site tyrosine changes a retaining sialidase into an inverting sialidase. *Biochemistry* 42, 12682–12690.

(19) Watson, J. N., Newstead, S., Dookhun, V., Taylor, G., and Bennet, A. J. (2004) Contribution of the active site aspartic acid to catalysis in the bacterial neuraminidase from *Micromonospora viridifaciens*. *FEBS Lett.* 577, 265–269.

(20) Newstead, S., Watson, J. N., Knoll, T. L., Bennet, A. J., and Taylor, G. (2005) Structure and mechanism of action of an inverting mutant sialidase. *Biochemistry* 44, 9117–9122.

(21) Watson, J. N., Newstead, S., Narine, A., Taylor, G., and Bennet, A. J. (2005) Two nucleophilic mutants of the *Micromonospora viridifaciens* sialidase operate with retention of configuration via two different mechanisms. *ChemBioChem* 6, 1999–2004.

(22) Taylor, N. R., and von Itzstein, M. (1994) Molecular modeling studies on ligand binding to sialidase from influenza virus and the mechanism of catalysis. *J. Med. Chem.* 37, 616–624.

(23) Islam, T., and von Itzstein, M. (2007) Anti-influenza drug discovery: Are we ready for the next pandemic? *Adv. Carbohydr. Chem. Biochem.* 61, 293–352.

(24) Indurugalla, D., Watson, J. N., and Bennet, A. J. (2006) Natural sialoside analogues for the determination of enzymatic rate constants. *Org. Biomol. Chem.* 4, 4453–4459.

(25) Narine, A. A., Watson, J. N., and Bennet, A. J. (2006) Mechanistic requirements for efficient enzyme-catalyzed hydrolysis of thiosialosides. *Biochemistry* 45, 9319–9326.

(26) Newstead, S. L., Watson, J. N., Bennet, A. J., and Taylor, G. (2005) Galactose recognition by the carbohydrate-binding module of a bacterial sialidase. *Acta Crystallogr. D* 61, 1483–1491.

(27) Shidmoosavee, F. S., Cheng, L., Watson, J. N., and Bennet, A. J. (2010) Brønsted analysis of an enzyme-catalyzed pseudo-deglycosylation reaction: Mechanism of desialylation in sialidases. *Biochemistry* 49, 6473–6484.

(28) Shidmoosavee, F. S., Watson, J. N., and Bennet, A. J. (2011) Sialic acid glycals are not transition state analogue inhibitors of influenza type A neuraminidase. *Nat. Chem. Biol.* In preparation.

(29) Watson, J. N., Indurugalla, D., Cheng, L., Narine, A. A., and Bennet, A. J. (2006) The hydrolase and transferase activity of an inverting mutant sialidase using non-natural  $\beta$ -sialoside substrates. *Biochemistry* 45, 13264–13275.

(30) Sambrook, J., Fritsch, E. F., and Maniatis, T. (1989) *Molecular cloning: A laboratory manual*, 2nd ed., Cold Spring Harbor Laboratory Press, Plainview, NY.

(31) Kuboki, A., Sekiguchi, T., Sugai, T., and Ohta, H. (1998) A facile access to aryl  $\alpha$ -sialosides: The combination of a volatile amine base and acetonitrile in glycosidation of sialosyl chlorides. *Synlett*, 479–482.

(32) Chou, D. T. H., Watson, J. N., Scholte, A. A., Borgford, T. J., and Bennet, A. J. (2000) Effect of neutral pyridine leaving groups on the mechanisms of influenza type A viral sialidase-catalyzed and the spontaneous hydrolysis reactions of  $\alpha$ -D-N-acetylneuraminides. *J. Am. Chem. Soc.* 122, 8357–8364.

(33) O'Reilly, D. R., Miller, L., and Luckow, V. A. (1994) *Baculovirus expression vectors: A laboratory manual*, Oxford University Press, New York.

(34) Colman, P. M., Varghese, J. N., and Laver, W. G. (1983) Structure of the catalytic and antigenic sites in influenza virus neuraminidase. *Nature* 303, 41–44.

(35) Ausubel, F. M. (1987) *Current protocols in molecular biology*, Greene Publishing Associates, John Wiley, Brooklyn, NY.

(36) Schowen, R. L. (1977) Solvent isotope effects on enzymic reactions. In *Isotope effects on enzyme-catalyzed reactions* (Cleland, W. W., O'Leary, M. H., and Northrop, D. B., Eds.) pp 64–99, University Park Press, Baltimore.

(37) Segel, I. H. (1975) *Enzyme kinetics: Behavior and analysis of rapid equilibrium and steady state enzyme systems*, Wiley, New York.

(38) Chan, J., Lu, A., and Bennet, A. J. (2011) Turnover is rate-limited by deglycosylation for *Micromonospora viridifaciens* sialidase-catalyzed hydrolyses: Conformational implications for the Michaelis complex. *J. Am. Chem. Soc.* 133, 1877–1884.

(39) Perugini, G., Falcicchio, P., Corsaro, M. M., Matsui, I., Parrilli, M., Rossi, M., and Moracci, M. (2006) Preparation of a glycosynthase from the  $\beta$ -glycosidase of the hyperthermophilic archaeon *Pyrococcus horikoshii*. *Biocatal. Biotransform.* 24, 23–29.

(40) Zechel, D. L., Reid, S. P., Stoll, D., Nashiru, O., Warren, R. A. J., and Withers, S. G. (2003) Mechanism, mutagenesis, and chemical rescue of  $\beta$ -mannosidase from *Cellulomonas fimi*. *Biochemistry* 42, 7195–7204.

(41) Alvarez, F. J., and Schowen, R. L. (1987) Mechanistic Deductions from Solvent Isotope Effects. In *Secondary and solvent isotope effects: Isotopes in organic chemistry*, pp 1–60, Elsevier, Amsterdam.

(42) Schowen, K. B., and Schowen, R. L. (1982) Solvent Isotope Effects on Enzyme Systems. *Methods Enzymol.* 87, 551–606.

(43) Sirimulla, S., Lerma, M., and Herndon, W. C. (2010) Prediction of Partial Molar Volumes of Amino Acids and Small Peptides: Counting Atoms versus Topological Indices. *J. Chem. Inf. Model.* 50, 194–204.

(44) Pierdominici-Sottile, G., and Roitberg, A. E. (2011) Proton transfer facilitated by ligand binding. An energetic analysis of the catalytic mechanism of *Trypanosoma cruzi* trans-sialidase. *Biochemistry* 50, 836–842.

(45) Li, Y.-K., Chir, J., and Chen, F.-Y. (2001) Catalytic mechanism of a family 3  $\beta$ -glucosidase and mutagenesis study on residue D147. *Biochem. J.* 355, 835–840.

(46) Withers, S. G., Rupitz, K., Trimbur, D., and Warren, A. J. (1992) Mechanistic consequences of mutation of the active site nucleophile Glu 358 in *Agrobacterium*  $\beta$ -glucosidase. *Biochemistry* 31, 9979–9985.

(47) Air, G. M., and Laver, W. G. (1989) The neuraminidase of influenza virus. *Proteins* 6, 341–356.

(48) Kleinedam, R. G., Kruse, S., Roggentin, P., and Schauer, R. (2001) Elucidation of the role of functional amino acid residues of the small sialidase from *Clostridium perfringens* by site-directed mutagenesis. *Biol. Chem.* 382, 313–319.

(49) Chien, C. H., Shann, Y. J., and Sheu, S. Y. (1996) Site-directed mutations of the catalytic and conserved amino acids of the neuraminidase gene, nanH, of *Clostridium perfringens* ATCC 10543. *Enzyme Microb. Tech.* 19, 267–276.

(50) Albohy, A., Li, M. D., Zheng, R. B., Zou, C. X., and Cairo, C. W. (2010) Insight into substrate recognition and catalysis by the human neuraminidase 3 (NEU3) through molecular modeling and site-directed mutagenesis. *Glycobiology* 20, 1127–1138.